

Spectral Study of the Galactic Ridge X-ray Emission with Suzaku

Ken EBISAWA,¹ Shigeo YAMAUCHI,² Yasuo TANAKA,³ Katsuji KOYAMA,⁴
Yuichiro EZOE,¹ Aya BAMBA,¹ Motohide KOKUBUN,¹ Yoshiaki HYODO,⁴
Masahiro TSUJIMOTO⁵ and Hiromitsu TAKAHASHI⁶

¹*Institute of Space and Astronautical Science/JAXA, 3-1-1 Yoshinodai, Sagamihara, Kanagawa 229-8510
ebisawa@isas.jaxa.jp*

²*Faculty of Humanities and Social Sciences, Iwate University, 3-18-34 Ueda, Morioka, Iwate 020-8550*

³*Max-Planck-Institut für extraterrestrische Physik, D-85740, Garching bei München, Germany*

⁴*Department of Physics, Graduate School of Science, Kyoto University, Sakyo-ku, Kyoto 606-8502*

⁵*Department of Astronomy & Astrophysics, Pennsylvania State University,
University Park, PA 16802, U.S.A.*

⁶*Department of Physical Science, Hiroshima University, 1-3-1 Kagamiyama,
Higashi-Hiroshima, Hiroshima 739-8526*

(Received 0 0; accepted 0 0)

Abstract

We have observed a typical Galactic plane field at $(l, b) = (28^\circ 46', -0^\circ 20')$ with Suzaku for 100 ksec to carry out a precise spectral study of the Galactic Ridge X-ray Emission (GRXE). The field is known to be devoid of X-ray point sources brighter than $\sim 2 \times 10^{-13} \text{ ergs s}^{-1} \text{ cm}^{-2}$ (2–10 keV), and already deeply observed with Chandra. Thanks to the low and stable background and high spectral resolution of Suzaku, we were able to resolve, for the first time, three *narrow* iron K-emission lines from low-ionized (6.41 keV), helium-like (6.67 keV), and hydrogenic ions (7.00 keV) in the GRXE spectrum. These line features constrain the GRXE emission mechanisms: The cosmic-ray ion charge exchange model or the non-equilibrium ionization plasma model are unlikely, since they require either broad emission lines or lines at intermediate ionization states. Collisional ionization equilibrium plasma is the likely origin for the 6.67 keV and 7.00 keV lines, while origin of the 6.41 keV line, which is due to fluorescence from cold material, is not elucidated. Low non-X-ray background and little stray-light contamination of Suzaku allowed us to precisely measure the absolute X-ray surface brightness in the direction of the Galactic plane. Excluding the point sources brighter than $\sim 2 \times 10^{-13} \text{ ergs s}^{-1} \text{ cm}^{-2}$ (2–10 keV), the total surface brightness on the Galactic plane is $\sim 6.1 \times 10^{-11} \text{ ergs s}^{-1} \text{ cm}^{-2} \text{ deg}^{-2}$ (2–10 keV), including the contribution of the cosmic X-ray background that is estimated to be $\sim 1.3 \times 10^{-11} \text{ ergs}$

$\text{s}^{-1} \text{cm}^{-2} \text{deg}^{-2}$.

Key words: Galaxy:disk—X-rays:diffuse background—X-rays:stars

1. Introduction

The Galactic plane has been known to be a source of hard (2–10 keV) X-ray emission since the 1980s (Worrall et al. 1982; Warwick et al. 1985; Koyama et al. 1986). Although most of the X-ray satellites have spent significant amounts of observing time to study the Galactic Ridge X-ray Emission (GRXE), its origin has not been elucidated yet. Whether the GRXE is truly diffuse emission or composed of numerous dim point sources remains inconclusive.

Ebisawa et al. (2001, 2005) studied a blank Galactic plane area at $(l, b) \approx (28.5, 0.0)$ with Chandra, consisting of two partially overlapping fields each exposed 100 ksec (sequence 900021 and 900125). They found that only 10 – 15 % of the observed 2–10 keV GRXE was resolved into point sources brighter than $\sim 3 \times 10^{-15} \text{ ergs s}^{-1} \text{ cm}^{-2}$. They also found that the point source surface density in the 2 – 10 keV band was not significantly higher than that at high Galactic latitudes, and therefore the majority of these hard X-ray sources is likely to be the background AGNs. On the other hand, numerous point sources were detected in the soft (< 2 keV) band which are considered to be nearby Galactic sources, hardly contributing to the 2 – 10 keV GRXE. Ebisawa et al. (2001, 2005) suggest that the number of Galactic hard X-ray sources starts to deplete ($\log N - \log S$ curve begins to saturate) around $\sim 3 \times 10^{-15} \text{ ergs s}^{-1} \text{ cm}^{-2}$ (2 – 10 keV), and they conclude that most of the GRXE has the diffuse origin.

Meanwhile, Revnivtsev et al. (2006) discovered a striking similarity between the global GRXE distribution and that of the near infrared (NIR) emission at $3.5 \mu\text{m}$. Since the NIR emission is considered to represent the stellar population, this spatial correlation is suggestive of the stellar origin of the GRXE. Assuming the low-luminosity X-ray source population based on the all-sky RXTE and ROSAT data of the sources in the solar neighborhood (Sazonov et al. 2006), Revnivtsev et al. (2006) proposed that the GRXE is ultimately resolved into point sources at $\sim 10^{-16} - 10^{-16.5} \text{ ergs s}^{-1} \text{ cm}^{-2}$ (2 – 10 keV). Revnivtsev and Sazonov (2007) claim that, using the same Chandra data as those of Ebisawa et al. (2005), $\sim 25\%$ of the GRXE in 1– 7 keV is accounted for by point sources brighter than $1.2 \times 10^{-15} \text{ ergs s}^{-1} \text{ cm}^{-2}$ (interstellar absorption corrected flux), and that there is no indication of saturation of the $\log N - \log S$ slope down to this flux limit. In order to test the point source origin, one would need more than an order of magnitude lower limiting flux than the current value. Currently only Chandra can make the required observations, which would have much deeper (> 1 Msec) exposures than those already carried out.

Another important property of the GRXE is its energy spectrum. It has been known from previous observations that the spectrum is hard (e.g, Valinia et al. 2000) and characterized by many intense emission lines from highly ionized ions of the abundant elements (e.g., Kaneda

et al. 1997). These emission lines, in particular the iron K-emission lines in 6–7 keV, can constrain the emission mechanism. Suzaku satellite is the best suited for this study, since it is equipped with the X-ray telescopes of large effective areas, and the focal plane detectors of superior spectral resolution. In addition, Suzaku’s low and stable background and small stray-light contamination enable us to measure the total surface brightness on the Galactic plane accurately, from which we can estimate the absolute GRXE flux by subtracting the contribution of the cosmic X-ray background. In this paper, we report the results of a 100 ksec observation of the GRXE with Suzaku for the same Galactic plane field as that of the Chandra observation by Ebisawa et al (2001, 2005).

2. Observation and Data Analysis

2.1. Observation

Suzaku (Mitsuda et al. 2007), the fifth Japanese X-ray satellite, was launched on July 10, 2005, and carries four X-ray CCD cameras (X-ray Imaging Spectrometers; XIS; Koyama et al. 2007a) at the foci of four X-ray telescopes (XRT; Serlemitsos et al. 2007) and the Hard X-ray Detector (HXD; Takahashi et al. 2007). The first Suzaku long exposure of the Galactic Ridge (sequence number 500009010) was carried out during the proprietary period for the Science Working Group, from Oct. 28 02:24 to Oct. 30 21:30, 2005, for 100 ksec. The pointing center was chosen exactly at the same position as the Chandra AO1 field (sequence number 900021), (RA,DEC)=(281°000, −4°070) (J2000) or $(l, b) = (28^\circ 463, -0^\circ 204)$. Since the XIS field of view ($17'8 \times 17'8$) is comparable to that of Chandra ACIS ($16'9 \times 16'9$), almost the same field was covered (figure 1).

In the present study, we concentrate on the results obtained from the XIS. There are four XIS sensors, XIS0 to XIS3, of which XIS1 carries the back-illuminated chip and all the rest have front illuminated chips. Although XIS1 has superior sensitivity and spectral resolution at low energies ($\lesssim 1$ keV), it suffers from a higher intrinsic background relative to the front-illuminated sensors. The Spaced-row Charge Injection (SCI) operation (Nakajima et al. 2007), which later became a regular operational mode, was not performed in the current observation. Processing version of the data used in this study is v.1.2.2.3, and the software version is heasoft 6.2.

During our observation, a transient source was found at (RA, DEC)=(281°034, −4°081), which is named Suzaku J1844–0404 (Yamauchi et al. 2007). To avoid contamination from the source, those events within a two-arcmin radius from the transient source are excluded in the following data analysis (figure 1). In addition, we exclude the region which contains a part of the supernova remnant G28.6–0.1 (Bamba et al. 2001; Ueno et al. 2003) (figure 1). Besides these two, no discrete/point sources brighter than $\sim 2 \times 10^{-13}$ ergs s $^{-1}$ cm $^{-2}$ (2–10 keV) were detected. In other words, point sources dimmer than $\sim 2 \times 10^{-13}$ ergs s $^{-1}$ cm $^{-2}$ (2–10

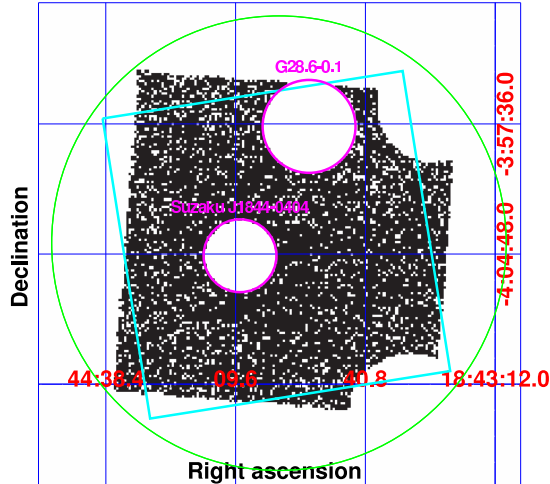


Fig. 1. The XIS0 sky image of the region selected for the present analysis. Calibration sources at the upper-right and lower-right corners are removed. In addition, the supernova remnant G28.6–0.1 (Bamba et al. 2001; Ueno et al. 2003; upper-circle in magenta), and the transient source Suzaku J1844-0404 (Yamauchi et al. 2006; lower-circle in magenta) are excluded. The overlapping square in cyan is the Chandra AO1 (sequence 900021) ACIS field of view. Assumed sky region to calculate the ARF (green circle with 12'6 radius) is also indicated.

keV), either Galactic or extragalactic, are necessarily included in the following GRXE spectral analysis.

2.2. Background Subtraction

The intrinsic (non X-ray) background is estimated using the XIS background database which was built from the long-term night Earth observations (Tawa et al. 2007)¹. For each XIS sensor, the data extraction region is defined by excluding the areas of calibration sources and the contamination sources (figure 1). The night Earth background spectra are constructed for the same detector region for each sensor. Since XIS intrinsic background is known to be dependent on the magnetic cut-off rigidity (COR)(Koyama et al. 2007a; Tawa et al. 2007), the night Earth background spectra were accumulated for several different COR bins separately, and properly weighted according to the COR distribution during the ridge observation.

Since the characteristics of the three front-illuminated chips are almost identical to each other, we combine the data from them and show the average spectrum (hereafter XIS023). In

¹ <http://www.astro.isas.jaxa.jp/suzaku/analysis/xis/nte>

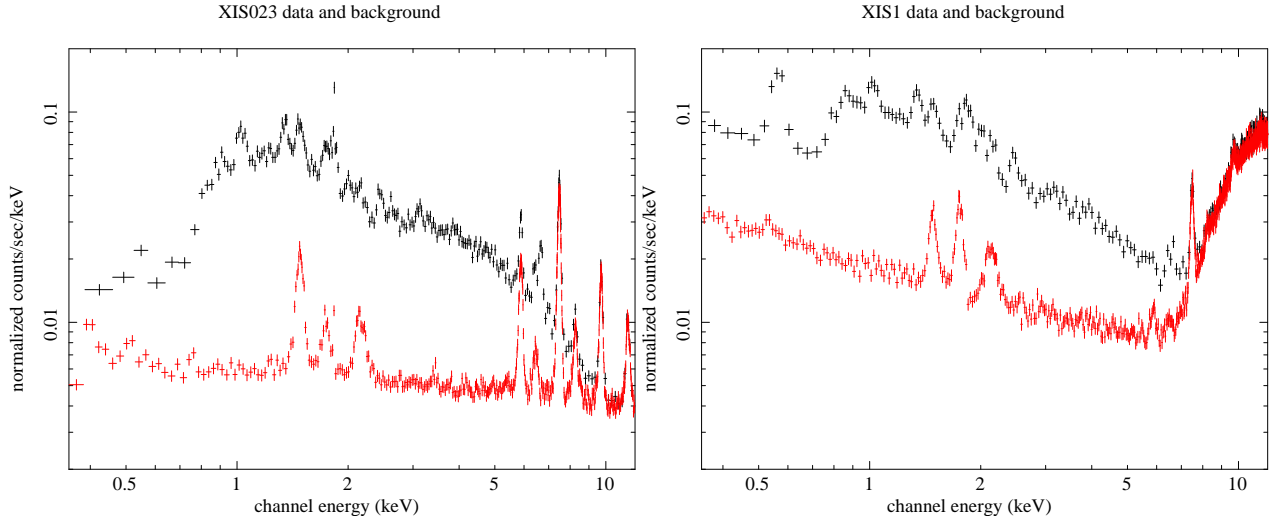


Fig. 2. The Galactic Ridge spectra (black; background is not subtracted) and particle background spectra (red) with XIS0, 2, 3 (three sensors averaged; left) and XIS1 (right).

figure 2, we show the observed energy spectra and the corresponding night Earth spectra for XIS023 (front-illuminated) and XIS1 (back-illuminated).

If we compare figure 2 with a corresponding (background dominated) figure by Chandra (e.g., figure 7 in Ebisawa et al. 2005), it is evident that Suzaku is much more sensitive to extended emission thanks to the large effective area and low background. Among four XIS sensors, XIS0, 2, 3 have much lower intrinsic background in 5 – 8 keV than XIS1, which is particularly advantageous for the study of the iron K-lines.

2.3. Telescope Response

The telescope response was calculated using the `xissimarfgen` tool via ray-tracing (Ishisaki et al. 2007). The assumed sky region of the input photons is a circle with 25.′2 diameter (0.139 deg^2), that corresponds to the diagonal of a CCD chip (figure 1). The uniformly distributed photons from the 0.139 deg^2 area are put into the simulator and the number of photons falling onto the selected detector area are calculated for each energy bin. Thus, the “Ancillary Response File” (ARF) is calculated with the unit of cm^2 . Using this ARF in spectral fitting together with the XIS response (“Redistribution Matrix File”; RMF) gives the diffuse spectral model in the unit of $\text{photons s}^{-1} \text{ cm}^{-2} \text{ keV}^{-1}$ per 0.139 deg^2 . In this paper, we give normalized flux in the unit of $\text{photons s}^{-1} \text{ cm}^{-2} \text{ deg}^{-2}$.

Suzaku XRT is known to have little stray-light contamination from outside of the field of view (Serlemitsos et al. 2007), in contrast to the similar type telescopes on-board ASCA where stray-light significantly affected the GRXE study (e.g., Kaneda et al. 1997). Consequently, together with the low/stable background, we are able to accurately measure the energy spectrum and surface brightness of the extended emission using Suzaku.

Table 1. Iron Line Parameters

Energy [keV]	6.41 ± 0.02	6.670 ± 0.006	7.00 ± 0.03
Intrinsic Gaussian width (1σ) [eV]	< 120	< 46	< 52
Flux [10^{-5} photons/s/cm ² /deg ²]	8 ± 2	25 ± 3	5 ± 2
Equivalent Width [eV]	80 ± 20	350 ± 40	70 ± 30

3. Results

3.1. Iron K-emission Lines

We are particularly interested in the iron K-energy band (~ 6.5 keV), since the iron line energies and the widths give us important clues for the GRXE emission mechanism. We use only the XIS023 spectrum to study iron lines, since XIS1 suffers from high background in this energy band (figure 2, right). The emission line feature is obvious in the XIS023 spectrum. We fitted the data in the 6 – 10 keV band with an absorbed bremsstrahlung model for the continuum and three Gaussian profiles with free intrinsic widths (energies allowed to be free around 6.4 keV, 6.7 keV and 7.0 keV), as well as the neutral K_β line whose energy, intrinsic width (1σ) and intensity are fixed at 7.06 keV, 10 eV and at 0.125 times the 6.4 keV line intensity, respectively (Kaastra & Mewe 1993). The fit above 6 keV is hardly affected by the hydrogen column density, which is fixed at the value constrained from the low energy model fitting ($N_H = 1.1 \times 10^{21}$ cm⁻²; see below). We got $kT = 3.9$ keV and $\chi^2=197.6$ with d.o.f.=213. In figure 3, we show the observed energy spectrum and the best-fit model. In table 1, the best-fit line parameters are given (errors quoted in this paper correspond to the 90 % confidence limits). We also tried a power-law continuum (photon-index=3.2) instead of the bremsstrahlung, but the line parameters hardly depended on the continuum model used.

It is noteworthy that three individual (near neutral, He-like and H-like) iron K-lines are clearly visible in the GRXE spectrum for the first time. Previously, these lines were only barely resolved with ASCA or Chandra because of their poorer energy resolutions (e.g., Kaneda et al. 1997; Tanaka 2002; Ebisawa et al. 2005), while the line fluxes and equivalent widths obtained with ASCA and Chandra are consistent with the present Suzaku values.

It is also important that we can constrain the intrinsic widths for the 6.67 keV line and 7.0 keV line, making reference to the 5.9 keV Mn-K calibration line (one sigma width ≈ 30 eV; Koyama et al. 2007b). Thus determined widths of the iron lines are consistent with 0.

3.2. Low Energy Lines

Next, we study low energy lines in the 0.4 – 4 keV band. Both XIS023 and XIS1 spectra are fitted simultaneously with the same parameter values except relative normalization, where we found XIS1 normalization is 1.03 times that of XIS023. Below, we show normalization values

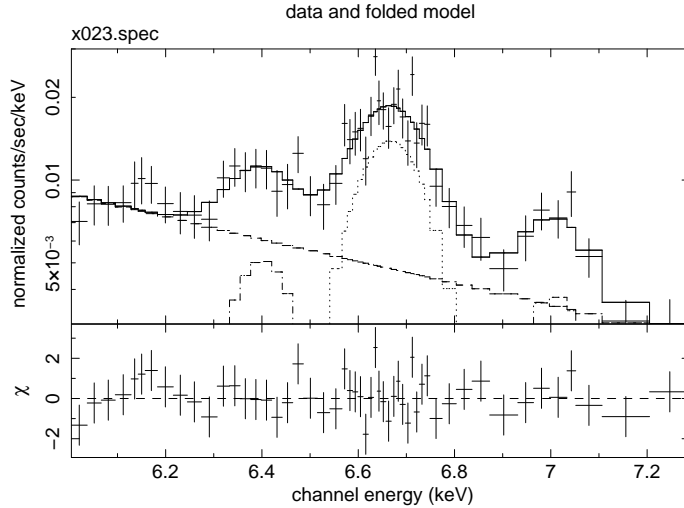


Fig. 3. Spectral fitting of the XIS023 spectrum in the iron K-line region with a power-law continuum and three narrow Gaussians.

derived from XIS023. We adopt an absorbed power-law for the continuum and 13 Gaussians in order to successfully reproduce the observed spectrum (figure 4), where we find choice of the continuum model hardly affects the line parameters. The best-fit photon-index and the hydrogen column density are 0.88 ± 0.03 and $N_H = (1.1 \pm 0.1) \times 10^{21} \text{ cm}^{-2}$, respectively. Note that these phenomenological values may not represent actual physical parameters, since origin of the continuum emission is presumably more complex. The fit was satisfactory with $\chi^2 = 1174$ for d.o.f=1102. Intrinsic line widths are not constrained besides the strongest OVII line (see below), thus we fixed them at $1\sigma = 5 \text{ eV}$. The best-fit line parameters and the most likely line identifications are given in table 2. The line flux is not corrected for interstellar absorption.

Basically, the same emission lines are detected from highly ionized heavy elements as previously observed with ASCA (Kaneda et al. 1997; Tanaka 2002) and Chandra (Ebisawa et al. 2005), but with much better resolution. Note that the strong OVII line at $0.560 \pm 0.03 \text{ keV}$ is most probably dominated by the forbidden line (0.561 keV) originated in the Earth’s magnetosheath caused by solar-wind charge exchange (see Fujimoto et al. 2007), since the line energy is not consistent with the OVII resonance line at 0.574 keV that is expected from the GRXE and/or the local hot plasma. Since the 0.560 keV line is so strong, it serves for the purpose of calibration; the 90 % upper-limit of the intrinsic line width (1σ) is constrained at 6 eV.

3.3. Total X-ray Flux on the Galactic Plane

As explained above, we successfully fitted the energy spectrum in 6 – 10 keV and 0.4 – 4 keV separately with a simple power-law continuum and Gaussian lines. However, it is not easy to find a model which can fit the observed spectrum in the entire energy range. Therefore, in

Table 2. Low energy model fitting parameters

Energy (keV)	Line Flux ^a	Equivalent Width (eV)	Identification
0.560±0.003	320 ± 50	346 ± 54	OVII f, 0.561 keV
0.647±0.024	7 ₋₇ ⁺¹³	9 ₋₉ ⁺¹⁷	OVIII, 0.653 keV
0.829±0.004	26 ± 7	40 ± 21	FeXVII, 0.826 keV
0.906±0.003	30 ± 7	49 ± 11	NeIX, 0.922 keV
1.021±0.002	36 ± 5	66 ± 9	NeX, 1.022 keV
1.342±0.003	18 ± 3	42 ± 7	MgXI, 1.352 keV
1.474±0.012	4.4 ± 2.5	11 ± 6	MgXII, 1.472 keV
1.843±0.003	22 ± 4	70 ± 13	SiXIII, 1.865 keV
1.997±0.009	7.6 ± 1.3	25 ± 4	SiXIV, 2.006 keV
2.444±0.004	21 ± 3	86 ± 12	SXV, 2.461 keV
2.624±0.009	8.5 ± 2.7	36 ± 11	SXVI, 2.622 keV
3.139±0.010	7.7 ± 2.4	39 ± 12	ArXVII, 3.140 keV
3.321±0.016	5.1 ± 2.4	27 ± 13	ArXVIII, 3.321 keV

^a10⁻⁵ photons s⁻¹ cm⁻² deg⁻².

order to determine the total flux in the direction of the Galactic plane in the standard energy band 2 – 10 keV, we furthermore fit the spectrum in 4 – 6 keV separately with simple power-law, and sum the contributions from the individual energy bands.

The 2 – 10 keV flux thus determined is 6.1×10^{-11} ergs s⁻¹ cm⁻² deg⁻² (XIS0, 2 and 3 average). Also, the 0.5 – 2 keV flux obtained from the low energy spectral fitting (previous section) is 1.1×10^{-11} ergs s⁻¹ cm⁻² deg⁻² (XIS0, 2 and 3 average), excluding the OVII forbidden line. Note that these fluxes include contribution of point sources dimmer than $\sim 2 \times 10^{-13}$ ergs s⁻¹ cm⁻² (2 – 10 keV), which are not resolved with Suzaku.

The Chandra fluxes calculated with the same condition are 7.4×10^{-11} ergs s⁻¹ cm⁻² deg⁻² (2 – 10 keV) and 9.7×10^{-12} ergs s⁻¹ cm⁻² deg⁻² (0.5 – 2 keV) (Ebisawa et al. 2005). The ~ 20 % difference in the 2 – 10 keV flux is due to systematic calibration uncertainty between Chandra and Suzaku, which has yet to be understood.

4. Discussion

4.1. Emission Mechanism of the GRXE

We have observed a typical Galactic plane region at $(l, b) \approx (28.46, -0.20)$ (= the Chandra AO1 deep field) with Suzaku. Thanks to the superior spectral resolution, the large effective area and the low background of Suzaku XIS, we obtained so far the best quality spectrum of the GRXE. For the first time, the iron K-line complex was clearly resolved into three individual peaks at 6.4 keV, 6.67 keV and 7.0 keV. Importantly, the line widths are also tightly

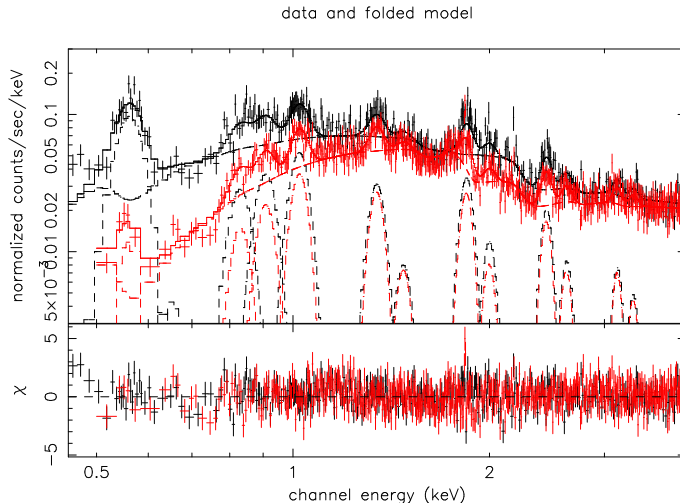


Fig. 4. Spectral fitting of the XIS1 (black) and XIS023 (red) spectra in the low energy band.

constrained to be less than ~ 50 eV (1σ).

The central energy of the He-like $K\alpha$ line, which is in fact a blend of the resonance, inter-combination and forbidden lines, is a good indicator of the plasma condition (see Koyama et al. 2007b). In the case of collisional ionization equilibrium (CIE), the centroid is 6.680–6.685 keV, depending on plasma densities and different plasma models (Koyama et al. 2007b). The peak energy is shifted downward if the plasma is in a non-equilibrium ionization (NEI) state. Using ASCA SIS, Kaneda et al. (1997) claimed to have detected a *single* narrow emission line at 6.61 ± 0.04 keV, that is significantly lower than what is expected in the CIE case, and suggested that the iron line is from a NEI plasma. Chandra observation by Ebisawa et al. (2005) also indicated a similar line center energy $6.52 \pm_{0.14}^{0.08}$ keV, if the line feature is fitted with a *single* Gaussian. Meanwhile, thanks to Suzaku’s superior sensitivity and energy resolution, we unambiguously detected the two separate lines at 6.41 keV and 6.670 keV, the flux of the former being one-third of that of the latter. The centroid of the two lines will be at 6.58 keV, and the 7.0 keV line is too weak to be detected with ASCA and Chandra. Hence, we consider that the lower He-like $K\alpha$ line energies previously reported by ASCA and Chandra were significantly affected by the presence of the 6.41 keV line, which was unresolved by these instruments.

Koyama et al. (2007b) determined the He-like $K\alpha$ line energy from the Galactic Center (GC) plasma as 6.680 ± 0.001 keV, which is consistent with the CIE plasma model. We obtained a very close value of 6.670 ± 0.006 keV, which does not show evidence of the NEI conditions. Thanks to the brightness of the GC plasma illuminating the entire CCD chip, Koyama et al. (2007b) were able to perform the chip-segment dependent Charge Transfer Inefficiency (CTI) correction, which effectively increased the iron line energies by several electron-volts. We cannot apply the same correction, since the Ridge emission is not so strong; however, if we consider the possible upward shift of the line energies due to this effect, our line energy completely agrees

with that from the GC and the CIE plasma. The observed H-like/He-like line intensity ratio (~ 0.2) is also consistent with that expected for a CIE plasma of $kT = 5 - 8$ keV.

Earlier, Tanaka et al. (2000) reported that, analyzing the ASCA data of the extended emission in the Galactic center region, the iron K-lines are significantly broadened with a width of ~ 70 eV. They suggested a possibility of the charge exchange process for the origin of the lines, where low-energy cosmic-ray iron ions will undergo charge exchange as they slow down in the interstellar space. They interpreted the finite line width as due to the bulk motion of the cosmic-ray ions. Tanaka (2002) pointed out the close similarity of the shape of the GRXE spectrum (at the same direction as the present one) with that around the Galactic center, and considered that the iron lines in the GRXE may as well be broadened, while this could not be examined with ASCA due to insufficient statistics.

The He-like $K\alpha$ line energy expected from the charge exchange process is 6.666 ± 0.005 keV (Wargelin et al. 2005), which is not clearly excluded from the present result 6.670 ± 0.006 keV unless the segment-dependent CTI correction is applied. However, our result supports that the He-like and H-like iron lines from the Galactic ridge are essentially narrow lines, which is against the line-broadening due to the cosmic-ray bulk motion and charge exchange. The Suzaku observation of the GC region also clearly refuted the broadening of the iron lines, as well as that the He-like $K\alpha$ line energy does not agree with that expected from the charge exchange (Koyama et al. 2007b). Therefore, we conclude that the charge exchange origin is quite unlikely for GRXE, as well as GC plasma.²

Thus, a CIE plasma is the most probable origin of the He-like and H-like iron $K\alpha$ lines. By the same token, the lower-energy lines from highly ionized ions of other abundant elements are considered to be thermal emission. However, the thermal structure of the plasma is not simple. As shown in Table 2, the H-like/He-like line intensity ratio is similar among different elements from Mg through Ar, and all roughly 0.3 – 0.5, and the same is true for Fe. This presumably requires a multi-temperature plasma.

There exist two alternative possibilities to explain the CIE plasma emission from the Galactic Ridge. The fundamental difference is whether such plasma is genuinely diffuse or gravitationally bound in the stellar sources. Consequently the ultimate questions are the following: (1) Does the superposition of all the point sources reproduce the observed GRXE spectrum, in particular, the complex emission line features? (2) Is the number of such Galactic point sources sufficient to explain the total GRXE flux?

As regards the origin of the 6.4 keV line, which is not emitted by the hot plasma but due to fluorescence from cold material, another explanation is required. Based on the diffuse

² The reason why Tanaka et al. (2000) obtained the line width of ~ 70 eV is still unclear. As written in their paper, the observed spectra from eight CCD chips were stacked with reference to the 6.7-keV line peak position, such that the line width after summation was minimized. One possibility is that the tuning of the energy scales among each other was not sufficient.

model, Valinia et al. (2000) proposed that interaction between the interstellar medium and cosmic supra/non-thermal electrons is responsible for the 6.4 keV line, as well as for the hard-tail observed above ~ 10 keV (Yamasaki et al. 1997; Valinia et al. 2000). On the other hand, superposition of numerous, different kinds of point sources may create such complex iron line spectra (Revnivtsev et al. 2006). In fact, quiescent cataclysmic variables are known to emit three iron lines, where the 6.4 keV line is due to reflection from the white-dwarf surfaces (e.g., Ezuka & Ishida 1999). Also, cataclysmic variables often reveal multi-temperature spectra with various emission lines as seen in GRXE.

4.2. Absolute flux of the GRXE

Excluding the point sources brighter than 2×10^{-13} ergs $\text{s}^{-1}\text{cm}^{-2}$ (2–10 keV), we have measured the total flux in the direction of the Galactic plane (including cosmic X-ray background) as 6.1×10^{-11} ergs $\text{s}^{-1} \text{cm}^{-2} \text{deg}^{-2}$ (2–10 keV), which is consistent with the Chandra measurement on the same region within 20 %. Currently, only ~ 15 % of the 2 – 10 keV of the total surface brightness is explained by the point sources (either Galactic or extragalactic) brighter than $\sim 3 \times 10^{-15}$ ergs $\text{s}^{-1}\text{cm}^{-2}$ (Ebisawa et al. 2005). In 1 – 7 keV, where Galactic point sources are more dominant, ~ 25 % of the total flux is resolved into point sources with interstellar absorption corrected fluxes higher than 1.2×10^{-15} ergs $\text{s}^{-1}\text{cm}^{-2}$ (Revnivtsev & Sazonov 2007).

For comparison, we estimate the cosmic X-ray background (CXB) flux seen through the Galactic plane. The 2–10 keV CXB flux determined from the high galactic region is $\sim 2 \times 10^{-11}$ ergs $\text{s}^{-1} \text{cm}^{-2} \text{deg}^{-2}$ (Moretti et al. 2003), where point sources dimmer than 8.0×10^{-12} ergs $\text{s}^{-1} \text{cm}^{-2}$ are included. In order to compare with our results where point sources brighter than 2.0×10^{-13} ergs $\text{s}^{-1} \text{cm}^{-2}$ are excluded, we subtract the cumulative flux of the sources between 2.0×10^{-13} ergs $\text{s}^{-1} \text{cm}^{-2}$ and 8.0×10^{-12} ergs $\text{s}^{-1} \text{cm}^{-2}$ using the model extragalactic $\log N - \log S$ curve by Moretti et al. (2003); thus we obtained the unabsorbed CXB flux $\sim 1.8 \times 10^{-11}$ ergs $\text{s}^{-1} \text{cm}^{-2} \text{deg}^{-2}$.

The hydrogen column density through the Galactic plane is estimated to be $\sim 6 \times 10^{22}$ cm^{-2} in this direction (Ebisawa et al. 2001), which attenuates the background CXB down to ~ 70 % in 2 – 10 keV, assuming a photon-index of 1.7. Consequently, $\sim 1.3 \times 10^{-11}$ ergs $\text{s}^{-1} \text{cm}^{-2} \text{deg}^{-2}$ is expected from the background CXB on the Galactic plane, which is ultimately resolved into individual AGNs. Chandra already resolved point-sources down to 3×10^{-15} ergs $\text{s}^{-1}\text{cm}^{-2}$, whose cumulative flux is $\sim 9 \times 10^{-12}$ ergs $\text{s}^{-1} \text{cm}^{-2} \text{deg}^{-2}$. Therefore, we see that a significant part of the dim hard Chandra sources is extragalactic. In fact, only ~ 20 % of the Chandra hard X-ray sources had near-infrared counterparts down to $K \approx 16$ (hence considered to be Galactic), whereas almost all the soft X-ray sources had counterparts (Ebisawa et al. 2005).

In conclusion, we measure the flux of the the Galactic Ridge X-ray emission as $\sim 4.8 \times$

10^{-11} ergs s $^{-1}$ cm $^{-2}$ deg $^{-2}$ (2 – 10 keV), excluding the Galactic and extragalactic sources brighter than 2×10^{-13} ergs s $^{-1}$ cm $^{-2}$ and the estimated contribution of dimmer extragalactic sources. How much fraction of this emission is ultimately resolved into Galactic point sources has been a long standing question (e.g., Worrall & Marshall 1983; Ottmann & Schmitt 1992; Mukai & Shiokawa 1992; Ebisawa et al. 2005; Revnivtsev et al. 2006; Revnivtsev & Sazonov 2007). A future ultra-deep Chandra observation on the Galactic Ridge is expected to give the answer.

4.3. Plasma Density Diagnostics of the GRXE

We obtained the GRXE flux (excluding the extragalactic sources) as $\sim 4.8 \times 10^{-11}$ ergs s $^{-1}$ cm $^{-2}$ deg $^{-2}$ (2 – 10 keV) in the direction of $(l, b) \approx (28^\circ 46, -0^\circ 20)$. Assuming that distance to the Galactic center is 8.5 kpc and radius of the Galactic disk 20 kpc, distance to the edge of the Galactic disk in this direction is ~ 25 kpc. Hence, we estimate the GRXE emissivity as $\sim 2.6 \times 10^{-29}$ erg s $^{-1}$ cm $^{-3}$ or $\sim 7.7 \times 10^{26}$ erg s $^{-1}$ pc $^{-3}$. Thermal bremsstrahlung emissivity is given as $\sim 2.4 \times 10^{-27} T^{1/2} N_e^2$ erg cm $^{-3}$ s $^{-1}$ (Zombeck 2007), thus if we assume uniformly distributed hot plasma with $T \approx 6 \times 10^7$ K, the electron density is $N_e \sim 1.2 \times 10^{-3}$ cm $^{-3}$, which is extremely tenuous.

The Galactic volume corresponding to 1 deg 2 in the direction of $(l, b) \approx (28^\circ 5, 0^\circ 0)$ is $\sim 1.6 \times 10^9$ pc 3 . If the GRXE is ultimately resolved into point sources such as cataclysmic variables or active binary stars, $\sim 10^5$ sources are expected per deg 2 (Revnivtsev et al. 2006). Hence the spatial density of such sources is $\sim 6.3 \times 10^{-5}$ pc $^{-3}$, and the average luminosity is $\sim 1.1 \times 10^{31}$ erg s $^{-1}$ per source. We estimate volume of the plasma associated with each point source as $(fR_\odot)^3$, where f is the scaling factor, ≈ 1 for active binaries and $\lesssim 0.01$ for cataclysmic variables (white dwarfs). In the case of magnetic cataclysmic variables, which is supposed to be responsible for hard ($\gtrsim 10$ keV) part of the GRXE (Revnivtsev et al. 2006), f is expected to be particularly small, since accretion flow is concentrated on the small magnetic pole regions. Again assuming $T \approx 6 \times 10^7$ K, we obtain $N_e \sim 4 \times 10^{10} f^{-3/2}$ cm $^{-3}$.

Thus, we see that the GRXE plasma densities expected for the diffuse case and the point source case are many orders of magnitude different, which is distinguishable from plasma diagnostics. In near future, if we could resolve the He-like $K\alpha$ complex into individual lines, we may constrain density of the plasma, hence origin of the plasma emission. As a matter of fact, the resonance line (w) at 6699 eV is always the strongest, whereas emissivity of the forbidden line (z) at 6634 eV and those of the inter-combination lines (x,y) at 6680 eV and 6665 eV are dependent on the plasma density. In the high density plasma, the forbidden line is not supposed to be observed, while in the low-density coronal limit, the forbidden line is stronger than the inter-combination lines. Such precise spectral observations with a few eV resolution would have been already possible with Suzaku XRS (Kelley et al. 2007), and will be certainly realized by future calorimeter missions such as NeXT (Inoue and Kunieda 2004).

5. Summary

We have observed the typical Galactic plane region at $(l, b) \approx (28^\circ 46', -0^\circ 20')$ (the Chandra AO1 deep field) with Suzaku for 100 ksec to carry out spectral study of the Galactic Ridge X-ray Emission (GRXE). We were able to, for the first time, resolve three narrow iron K-emission lines with different ionization states from the GRXE, which constrains the GRXE emission models. Collisional ionization equilibrium plasma is the likely origin of the He-like and H-like $K\alpha$ lines, while origin of the 6.41 keV line is not elucidated. Excluding the point sources brighter than 2×10^{-13} ergs $s^{-1} cm^{-2}$ (2–10 keV), total observed flux in the direction of the Galactic plane (including cosmic X-ray background) is $\sim 6.1 \times 10^{-11}$ ergs $s^{-1} cm^{-2} deg^{-2}$ (2–10 keV), among which $\sim 4.8 \times 10^{-11}$ ergs $s^{-1} cm^{-2} deg^{-2}$ is considered to be Galactic. In order to discriminate the point source origin and diffuse origin of the GRXE, as an alternative of the Chandra ultra-deep observation, we propose plasma density diagnostics by resolving He-like iron line complex, which will be made possible by future X-ray micro-calorimeter missions.

6. Acknowledgement

We acknowledge all the Suzaku team members for having made this observation and study available. In particular, we thank Dr. Greg Brown and Prof. Manabu Ishida for useful comments on plasma diagnostics.

References

- Bamba, A., Ueno, M., Koyama, K., & Yamauchi, S. 2001, PASJ, 53, L21
Ebisawa, K., Maeda, Y., Kaneda, H., & Yamauchi, S. 2001, Science, 293, 1633
Ebisawa, K., et al. 2005, ApJ, 635, 214
Ezuka, H., & Ishida, M. 1999, ApJS, 120, 277
Fujimoto, R. et al. 2007, PASJ, 59, S133
Inoue, H. & Kunieda, H. 2004, Advances Space Research, 34, 2628
Ishisaki Y. et al. 2007, PASJ, 59, S113
Kaastra, J. S. & Mewe, R. A&A, 1993, 97, 443
Kaneda, H., Makishima, K., Yamauchi, S., Koyama, K., Matsuzaki, K., & Yamasaki, N. Y. 1997, ApJ, 491, 638
Koyama, K., Makishima, K., Tanaka, Y., & Tsunemi, H. 1986, PASJ, 38, 121
Kelley, R. L., et al. 2007, PASJ, 59, S77
Koyama, K., et al. 2007a, PASJ, 59, S23
Koyama, K., et al. 2007b, PASJ, 59, S245
Mitsuda, K., et al. 2007, PASJ, 59, S1
Moretti, A., Campana, S., Lazzati, D., & Tagliaferri, G. 2003, ApJ, 588, 696
Mukai, K., & Shiokawa, K. 1993, ApJ, 418, 863
Nakajima, H., et al. 2007, PASJ, this volume

- Ottmann, R. & Schmitt, J. H. M. M. 1992, *A&A*, 256, 421
- Revnivtsev, M., Sazonov, S., Gilfanov, M., Churazov, E., & Sunyaev, R. 2006 *A&A*, 452, 169
- Revnivtsev, M., & Sazonov, S. 2007, *A&A*, 471, 159
- Sazonov, S., Revnivtsev, M., Gilfanov, M., Churazov, E., & Sunyaev, R. 2006, *A&A*, 450, 117
- Serlemitsos, P., et al. 2007, *PASJ*, 59, S9
- Tanaka, Y., Koyama, K., Maeda, Y., & Sonobe, T. 2000, *PASJ*, 52, L25
- Tanaka, Y. 2002, *A&A*, 382, 1052
- Takahashi, T., et al. 2007, *PASJ*, 59, S35
- Tawa, N., et al. 2007, *PASJ*, this volume
- Ueno, M., Bamba, A., Koyama, K., & Ebisawa, K. 2003, *ApJ*, 588, 338
- Valinia, A., et al. 2000, *ApJ*, 543, 733
- Wargelin, B. J., Beiersdorfer, P., Neill, P. A., Olson, R. E., & Scofield, J. H. 2005, *ApJ*, 634, 687
- Warwick, R. S., et al. 1985, *Nature*, 317, 218.
- Worrall, D. M., et al. 1982, *ApJ*, 255, 111
- Worrall, D. M. & Marshall, F. E. 1983, *ApJ*, 267, 691
- Yamasaki, N. Y., et al. 1997, *ApJ*, 481, 821
- Yamauchi, S., et al. 2007, 59, S215
- Zombeck, M. V. 2007, "Handbook of Space Astronomy and Astrophysics", Third Edition, Cambridge University Press